Low Complexity PAPR Reduction Techniques for Clipping and Quantization Noise Mitigation in Direct-Detection O-OFDM Systems

Laia Nadal[a], Michela Svaluto Moreolo[a], Josep M. Fàbrega[a], Gabriel Junyent[a,b]

[a] *Centre Tecnològic de Telecomunicacions de Catalunya, 08860 Castelldefels (Barcelona), Spain. (e-mail: laia.nadal@cttc.es).*
[b] *Universitat Politècnica de Catalunya, 08034 Barcelona, Spain.*

Abstract

We present different distortionless peak-to-average power ratio (PAPR) reduction techniques that can be easily applied, without any symmetry restriction, in direct-detection (DD) optical orthogonal frequency division multiplexing (O-OFDM) systems based on the fast Hartley transform (FHT). The performance of DD O-OFDM systems is limited by the constraints on system components such as digital-to-analog converter (DAC), analog-to-digital converter (ADC), the Mach-Zehnder modulator (MZM) and electrical amplifiers. In this paper, in order to relax the constraints on these components, we propose to symmetrically clip the transmitted signal and apply low complexity (LC) distortionless PAPR reduction schemes able to mitigate, at the same time, PAPR, quantization and clipping noise. We demonstrate that, applying LC-selective mapping (SLM) without any additional transform block, the PAPR reduction is 1.5 dB with only one additional FHT block using LC-partial transmit sequence (PTS) with random partitions; up to 3.1 dB reduction is obtained. Moreover, the sensitivity performance and the power efficiency are enhanced. In fact, applying LC PAPR reduction techniques with one additional transform block and a 6 bit DAC resolution, the required receiver power for 8 dB clipping level and for a 10^{-3} BER is reduced by 5.1 dB.

Keywords: Fast Hartley transform, optical OFDM, peak to average power ratio, selective mapping, partial transmit sequence, direct-detection.

1. Introduction

Orthogonal frequency division multiplexing (OFDM) has been introduced in optical communications systems as it has the capability to provide flexible high-capacity transmission and to cope with dispersion impairments, thanks to the digital signal processing (DSP) at the transceivers and the multicarrier modulation <1>, <2>. High order modulation formats can be used for increasing the system spectral efficiency and unique scalability to high-speed transmission is achieved, resulting suitable to access, metro and long-haul optical networks. Direct-detection (DD) and coherent detection are two different implementations for receiving the OFDM signal through the optical channel. DD optical OFDM (O-OFDM) is a cost effective solution using simpler transmitter and receiver architectures than coherent schemes at expenses of the spectral efficiency and receiver sensitivity. When real-valued OFDM signals are transmitted, the modulation format is also called discrete multitone (DMT). A typical transmitter configuration uses a Mach-Zehnder modulator (MZM) and a single digital-to-analog converter (DAC). Additionally, in reception the local oscillator is not required and only one photodetector and an analog-to-digital converter (ADC) are needed to recover the signal. The signal processing in the DMT transmitter/receiver is based on the fast Fourier transform (FFT), forcing the Hermitian symmetry (HS) on the input symbols <3>. In <4>, an alternative transform to the FFT has been proposed for optical DMT systems: the fast Hartley transform (FHT). The FHT is a real trigonometric transform that gives real data when the input signal is mapped into a real constellation, such as binary phase-shift keying (BPSK) or M-ary pulse amplitude modulation (M-PAM), where M is the constellation size. The FHT allows simplifying the DSP, as it has the same routine in transmission and reception and does not require to implement the HS. Hence, as no symmetry constraint is required, all the subcarriers are filled with data, whereas, when the FFT is used, only half of the subcarriers carry information <3>. Both transforms have similar complexity and the same performance in terms of spectral efficiency and bit error rate (BER) <4; 5>. The transform kernels of the FFT and the FHT only differ for the imaginary unit, as the real and imaginary parts of the FFT coincide with the even and the negative odd parts of the FHT, respectively. Due to the kernel structure, the mirror-symmetric sub-bands of the FHT ensure subcarriers orthogonality, resulting in a suitable basis for OFDM modulation. The FHT is particularly attractive for the processing of real signals, as required

for example in high-speed and ultra-wideband DMT systems <6; 7; 8> or in DD O-OFDM systems for cost-effective implementation, using intensity modulation (IM), simplified electronic design and simple commercial components <4>. The range of applications is wide, including different network segments and different optical channel types, spanning from standard single mode fiber to optical wireless or optical interconnects <1; 3>. Moreover, the FHT processing enables the design of novel adaptively modulated O-OFDM schemes and low-complex adaptive transponders with variable bandwidth and bit rate <9; 5>.

The main drawback of OFDM is the high peak-to-average power ratio (PAPR). Occasionally, the transmitted signal exhibits very high peaks that can cause intermodulation among the subcarriers due to the nonlinearities of devices, such as MZM, ADC, DAC, and the fiber. The OFDM signal must be allocated in the linear part of the transfer function of the MZM. This can be controlled with the selection of the MZM bias point. However, the presence of high PAPR can introduce distortion. Furthermore, the dynamic range of DAC and ADC must be adjusted in order to accommodate the OFDM signal and avoid signal distortion. Hence, they must ensure a dynamic range up to the value of the PAPR, which implies very high values. Symmetrically clipping the signal is a possible solution to cope with these issues. It consists of limiting the amplitude of the transmitted signal to a maximum allowed value. However, clipping the signal causes distortion and results in clipping noise, which degrades the system performance <10>. On the other hand, the limited bit resolution of the DAC and ADC introduces quantization noise to the system. Different PAPR reduction techniques have been proposed in the literature to mitigate the PAPR in wireless <11; 12; 13; 14; 15> and optical systems <10; 16; 17; 18; 19; 20>. Some of them cause data rate loss due to the need of transmitting side information for the correct reconstruction of the signal. Whereas other can cause signal distortion or power increase.

In this paper, we present distortionless techniques for minimizing the PAPR, clipping and quantization noise in DD O-OFDM systems based on the FHT. Specifically, we propose low complexity (LC) selective mapping (SLM), partial transmit sequence (PTS) and precoding schemes in order to also reduce the required resources using simple and cost-effective architectures for the design of real-time transceivers scalable to high-speed transmission. As a result, the dynamic range of the converters can be adjusted to a lower value and the nonlinearity impairment caused by the electronic and optoelectronic devices can be reduced. We evaluate the performance in IM/DD systems

for cost-sensitive applications. However, the PAPR reduction is achieved by digital signal processing (DSP) at the transmitter and thus it is independent from the optical transmission system. So that, the proposed techniques can find application in other optical systems adopting transponders based on FHT, such as DD O-OFDM using linear field modulation for long-haul transmission.

The paper is organized as follows: in section 2, the O-OFDM system based on the FHT is described and the problem of PAPR, clipping and quantization noise is introduced. In section 3, an overview of PAPR reduction techniques that have been applied in optical communications is provided. Then, distortionless PAPR reduction techniques and LC schemes are proposed to be applied to the FHT-based DSP. The section ends with the PAPR performance of the analyzed techniques. In section 4, the sensitivity performance of DD O-OFDM using the FHT is compared to FFT-based systems; then an analysis of the system performance including PAPR reduction is presented. Specifically, in order to characterize the transceivers, we evaluate the back-to-back (B2B) system, first considering the quantization noise, due to the limited bit resolution of the converters, and then the clipping noise at the varying of the clipping level. Finally, we present the sensitivity performance of the B2B system affected by both quantization and clipping noise using the proposed techniques. The conclusions are drawn in section 5.

2. FHT-based O-OFDM system: PAPR, clipping and quantization

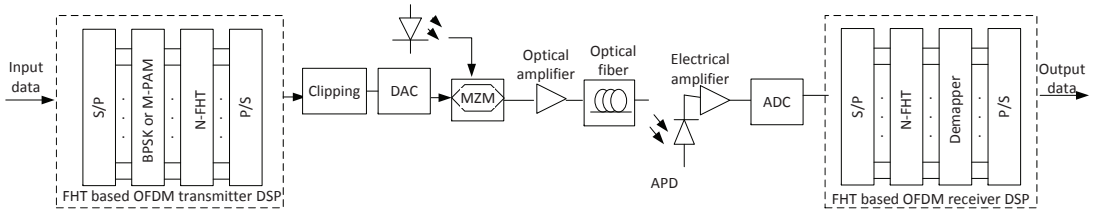

Figure 1: Block diagram of a DD O-OFDM system based on the FHT.

The proposed DD O-OFDM system based on the FHT is indicated in Fig. 1. The input data are parallelized and mapped into BPSK or M-PAM format. The resulting symbols are fed into an FHT of N points and then the modulated signal is serialized. Finally, it is symmetrically clipped and digital-to-analog converted. The resulting signal is then modulated with a

MZM. The modulated signal is transmitted over the optical channel. At the receiver side, the signal is photodetected with an avalanche photo-detector (APD), electrically amplified and analog-to-digital converted. Finally, the OFDM demodulation is performed including, serial-to-parallel conversion, FHT processing, demapping and serialization. Moreover, when an optical link is considered, equalization and synchronization should also be implemented at the receiver to correctly recover the transmitted data <21>. The transmitted discrete signal, x_m can be written as

$$x_m = \frac{1}{\sqrt{N}} \sum_{n=0}^{N-1} X_n cas(2\pi mn/N) \quad 0 \leq m \leq N-1, \tag{1}$$

where $cas(2\pi mn/N) = cos(2\pi mn/N) + sin(2\pi mn/N)$, N is the number of subcarriers of the FHT and X_n is the $n-th$ element of the input vector $\mathbf{X} = [X_0\ X_1\ X_2\ ...\ X_{N-1}]^T$. When N subcarriers are added in phase a high peak appears, whose power can be N times the average power. The ratio between the maximum peak power and the average power of the OFDM frame is defined as the signal PAPR:

$$PAPR = \frac{\max\limits_{0 \leq m \leq N-1} |x_m|^2}{E[|x_m|^2]}. \tag{2}$$

The theoretical limit of PAPR (in dB) can be derived from equation (2), giving

$$PAPR = 10 \log_{10} N, \tag{3}$$

and it only depends on the number of subcarriers <22>. For example, the theoretical maximum of the PAPR in a system with $N = 256$ subcarriers is 24 dB. However, this high value rarely occurs.

One common technique that is used to measure the PAPR is the complementary cumulative distribution function (CCDF), defined as

$$CCDF = P_r(PAPR > PAPR_0). \tag{4}$$

This function gives the probability that the PAPR exceeds a threshold $PAPR_0$. For calculating the PAPR of the continuous analog signal, Nyquist sampling rate can be used. However, it can occur that the maximum value of the O-OFDM signal may not be included in the sampled points of the

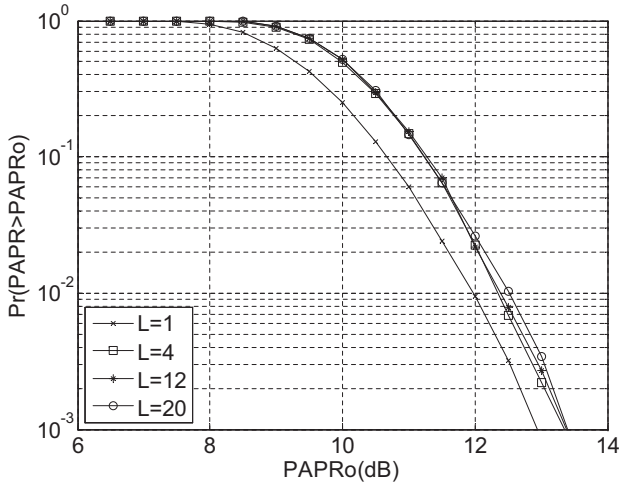

Figure 2: CCDF of O-OFDM based on FHT ($N = 256$) for different values of oversampling factor.

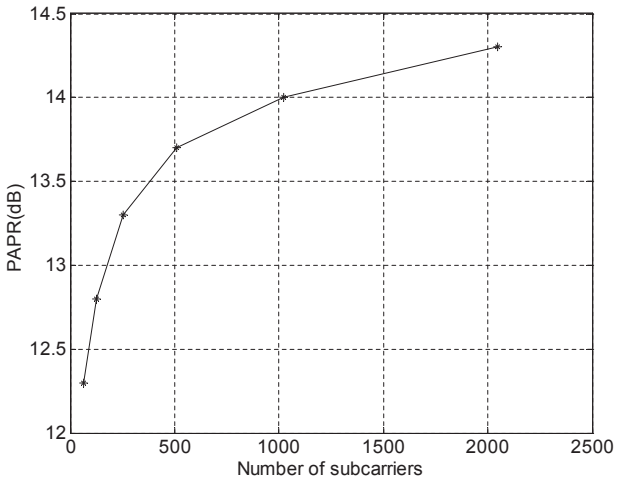

Figure 3: PAPR as a function of the number of subcarriers in FHT-based O-OFDM system at a CCDF of 0.1%. The oversampling factor is fixed at 4.

digital version. Therefore, an oversampling factor (L) is needed to consider the missing peaks. The oversampled time domain signal can be written as

$$\tilde{x}_m = \frac{1}{\sqrt{LN}} \sum_{n=0}^{LN-1} X_n cas(2\pi mn/(LN)) \quad 0 \leq m \leq LN-1. \tag{5}$$

The PAPR of the L times oversampled time domain signal, can be therefore calculated as

$$PAPR = \frac{\max\limits_{0 \leq m \leq NL-1} |\tilde{x}_m|^2}{E[|\tilde{x}_m|^2]}. \tag{6}$$

According to <23>, a fourfold oversampling factor ($L = 4$) is enough to consider the missing peaks when the FFT is used. Figure 2 shows the CCDF varying the oversampling factor L when the FHT is used. Fig. 2 shows that PAPR increases by about 0.5 dB when the oversampling factor is set to 4 in comparison with the case of no oversampling, i.e. $L = 1$. Whereas if the signal is oversampled with greater L factor of 12 or 20, the CCDF of the PAPR is almost the same as the one with $L = 4$. The PAPR also increases with the number of subcarriers, as shown in Fig. 3. When the number of subcarriers is set to $N = 256$ the probability that the PAPR exceeds 13.3 dB is less than 0.1% whereas with $N = 2048$ the PAPR increases by about 1 dB.

Symmetrically clipping is used to limit the high peaks of power that can occur in OFDM signals. The symmetrically clipped digital OFDM signal can be represented by

$$\hat{x}_m = \begin{cases} x_m, & |x_m| \leq B \\ \\ B \cdot sign(x_m), & |x_m| > B \end{cases} \tag{7}$$

where B is the maximum allowed signal amplitude and it is defined as k times the standard deviation of the signal ($B = k\sqrt{E[|x(m)|^2]}$) <4>. The clipping level (C) is defined in decibels as

$$C = 10 \cdot \log_{10}\left(\frac{B^2}{E[|x_m|^2]}\right), \tag{8}$$

where $E[|x_m|^2]$ denotes the average signal power of the transmitted signal. The clipped signal is normalized to a factor of $2B$, which is the peak-to-peak signal amplitude, in order to be adjusted to the dynamic range of the MZM <24>. Usually, the value of the clipping level is 7 dB <3>. However, when high order modulation formats are used, 7 dB is not enough to guarantee a BER lower than 10^{-3}. In fact, as clipping is a memoryless nonlinearity, it introduces signal distortion, which results in clipping noise. Higher clipping level values can be applied to the signal for reducing the clipping

noise at the expenses of increasing the electrical power of the signal <3>, <4>. Additionally, in the OFDM system, the quantization effects due to the digital-to-analog conversion must be also taken into account. According to <10> and using a uniform quantizer, we consider a step size Δ defined as $\Delta = 2B/(2R-1)$. R is the number of bits of the quantizer that corresponds to the number of binary digits used to represent each sample. The digital signal is quantized using $2R$ amplitude levels ($-B$, B and $-B + q\Delta$ with $q = 1, 2, ..., 2R-2$).

The optimization problem that is tackled in this paper is the minimization of the OFDM signal PAPR, specified by equation (6), in order to limit the signal distortion due to the clipping and to relax the DAC requirements.

3. PAPR reduction techniques

The problem of PAPR minimization can be solved using an exhaustive search. However, for a feasible system implementation in optical communications, the set of possible solutions must be limited, resulting in a suboptimal solution. Different PAPR reduction techniques have been proposed, in the literature, for optical communications <10; 16; 17; 18; 19; 20>. Clipping is the simplest PAPR reduction technique. However, as observed in section 2, it introduces clipping noise <10>. Active constellation extension (ACE), tone reservation (TR) and tone injection (TI) are another group of PAPR reduction techniques that achieve high PAPR reduction at expenses of high computational complexity and power increase. ACE consists of solving a convex optimization problem to find the optimum or suboptimum extension of the constellation points for minimizing the distance between them and thus reducing the PAPR <16>. TR and TI are based on adding a data-block-dependent time domain signal to reduce the PAPR. So in order to find the data-block that has the best performance, also for these techniques a convex optimization problem must be solved <18>. SLM, interleaving and PTS are distortionless PAPR reduction techniques that consist of finding an alternative representation of the signal that minimizes the PAPR, by adding transform blocks at the transmitter. In <17>, these techniques have been first proposed by the authors and analyzed in AWGN for IM/DD systems based on the FHT. Coding is another distortionless technique that consists of using codewords to reduce the PAPR. There is a wide range of alternative codewords such as Trellis shaping <12> or Alamouti space-time coding <13>. However, as coding techniques require an exhaustive search to find

the best codes, its implementation is very limited when a large number of subcarriers are used. Furthermore, their application to optical systems is limited due to the required complex digital processing at the transmitter. Precoding is a simpler type of coding that consists of multiplying the signal by a matrix to reduce the autocorrelation of the input sequence and thus the PAPR <20>. The precoding matrices can be based on the Hadamard transform <14> or the discrete cosine transform <15>. In this section, we propose to use distortionless PAPR reduction techniques that can be easily applied to O-OFDM systems based on the FHT with simplified DSP, allowing the implementation of low-complexity schemes.

3.1. Distortionless PAPR reduction techniques

Here, SLM, interleaving, PTS and precoding with Hadamard transform are used to design the FHT-based DSP with PAPR reduction capability.

3.1.1. Selective mapping

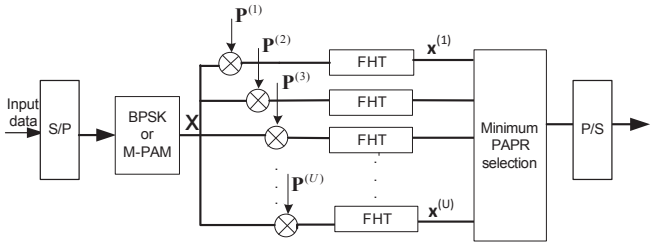

Figure 4: Block diagram of SLM PAPR reduction technique using U transform (FHT) blocks in order to create U different signal representations.

SLM consists of generating alternative OFDM frames representing the same information <25>. Each mapped input vector is multiplied by different vectors $\mathbf{P}^{(u)}$ with $u = 1, 2, ..., U$, where U is the number of FHT transform blocks and equal to the number of signal representations. The FHT is applied to the different signal representations, and the $\mathbf{P}^{(u)}$ that provides the minimum PAPR (i.e. equation (6)) is selected. Figure 4 shows the block diagram of SLM technique. $\mathbf{P}^{(u)}$ has N elements belonging to the set $\{\pm 1\}$, as real data are needed. In order to include the unmodified signal in the set of possible signal representations, all the elements of the first encoding vector $\mathbf{P}^{(1)}$ are set to one, so that $\mathbf{X}^{(1)} = \mathbf{X} \cdot \mathbf{P}^{(1)} = \mathbf{X}$ (see Fig. 4). The choice of these vectors is not restricted to any symmetry constraint. Increasing the

number U of signal representations increases the peak power reduction, but also the number of FHT blocks and thus the hardware resources needed for the system implementation. SLM requires $\log_2(U)$ bits of side information for the correct frame reception <11>. Using 4 transform blocks, only 2 bits are required to transmit side information to the receiver. This side information can be carried using 2 pilot tones and this overhead is negligible when compared with DMT systems based on the FFT, where the first and the Nyquist frequencies are set to zero to implement the HS.

3.1.2. Interleaving

Interleaving technique consists of permuting or reordering the original data to create different sequences that carry the same information; then the one that provides the minimum PAPR is selected <26>. The original input data vector with N components $\mathbf{X} = [X_0\ X_1\ ...\ X_n\ ...\ X_{N-1}]^T$ becomes $\mathbf{X'} = [X_{\varphi(0)}\ X_{\varphi(1)}\ ...\ X_{\varphi(n)}\ ...\ X_{\varphi(N-1)}]^T$, where the indexes of the vector elements are related by the one-to-one mapping $(n) \rightarrow (\varphi(n))$ and $\varphi(n) \in \{0, 1, ..., N-1\}$ for all n. Also in this case, U number of FHT blocks are required, where U denotes the number of interleavers. Increasing the number of interleavers enhance the system performance at expenses of higher computational complexity. In the particular case of $U = 4$, the required side information is $\log_2 U = \log_2 4 = 2$ bits.

3.1.3. Partial transmit sequence

The main idea of PTS technique is to divide the original frame into different subvectors $\mathbf{X}^{(v)}$ with $v = 1, 2, ..., V$ <27>, where V represents the number of required FHT blocks. These subvectors are created such that all the subcarriers positions, which are represented in other subvectors, are set to zero. The total number of zeros at the input of each FHT block is $(V-1)N/V$. A possible choice for the vector partitioning is based on adjacent selection, whereas another implementation is based on a random selection of the subvectors <28>. For example, in the case of $V = 2$ and $N = 8$, the resulting vectors $\mathbf{X}^{(v)}$, obtained after adjacent partitioning $\mathbf{X} = [X_0\ X_1\ X_2\ X_3\ X_4\ X_5\ X_6\ X_7]^T$, is $\mathbf{X}^{(1)} = [X_0\ X_1\ X_2\ X_3\ 0\ 0\ 0\ 0]^T$ and $\mathbf{X}^{(2)} = [0\ 0\ 0\ 0\ X_4\ X_5\ X_6\ X_7]^T$; whereas possible random partitions of $\mathbf{X}$ are $\mathbf{X}^{(1)} = [X_0\ 0\ X_2\ X_3\ 0\ 0\ 0\ X_7]^T$ and $\mathbf{X}^{(2)} = [0\ X_1\ 0\ 0\ X_4\ X_5\ X_6\ 0]^T$. Once the subvector partition is done, the FHT is performed and then the output is multiplied by the components of a weighting vector $\mathbf{p}^{(u)}$. To find the $\mathbf{p}^{(u)}$ that minimizes the PAPR of signal $\mathbf{F}(\mathbf{p}^{(u)})$ an exhaustive search is performed. Finally, the signal is recombined and transmitted using the

optimum $\mathbf{p}^{(u)}$. Due to the linearity of the FHT, we can write

$$\mathbf{F}(\mathbf{p}^{(u)}) = FHT\{\sum_{v=1}^{V} p_v^{(u)} \cdot \mathbf{X}^{(v)}\}$$

$$= \sum_{v=1}^{V} p_v^{(u)} \cdot FHT\{\mathbf{X}^{(v)}\} = \sum_{v=1}^{V} p_v^{(u)} \cdot \mathbf{x}^{(v)} \qquad u = 1, ..., U. \tag{9}$$

The elements of $\mathbf{p}^{(u)}$ are real values in the set $\{\pm 1\}$, where $p_1^{(u)}$ can be set

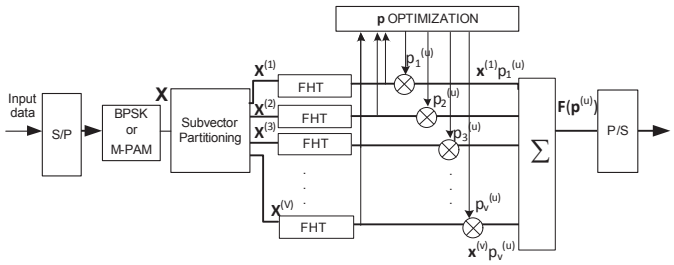

Figure 5: Block diagram of PTS PAPR reduction technique using V transform (FHT) blocks.

to 1 reducing the complexity of the optimization process without any loss of performance <27>. All the elements of $\mathbf{p}^{(1)}$ are set to 1, in order to consider the original vector. Therefore, the total number of optimization vectors is $2^{(V-1)}$ and it coincides with the total number of signal representations U. The required side information is $(V-1)\log_2(W)$ bits, where W represents the number of possible different values that the components of the vector $\mathbf{p}^{(u)}$ can assume. For example, in the case that the $\mathbf{p}^{(u)}$ components are in the set $\{\pm 1\}$ ($W = 2$) and using 4 FHT blocks ($V = 4$), the required side information is 3 bits. Compared with SLM and interleaving with 4 FHT blocks, PTS needs one additional bit to carry side information.

3.1.4. Precoding with the Hadamard transform

Precoding is another alternative distortionless PAPR reduction technique that consists of multiplying the vector $\mathbf{X}$ by a precoding matrix. Different precoding matrices can be used to reduce the PAPR. Here, we propose to use the Hadamard matrix for optical systems, as it is very easy to compute. The Hadamard transform is based on the Hadamard square matrix ($\mathbf{H}_N$) of dimensions $N \times N$, which elements are +1 or -1 <14>. The Hadamard

matrix of 1, 2 and N orders are:

$$H_1 = (1); \quad \mathbf{H}_2 = \frac{1}{\sqrt{2}} \begin{pmatrix} 1 & 1 \\ 1 & -1 \end{pmatrix}$$
$$\mathbf{H}_N = \frac{1}{\sqrt{N/2}} \begin{pmatrix} \mathbf{H}_{N/2} & \mathbf{H}_{N/2} \\ \mathbf{H}_{N/2} & -\mathbf{H}_{N/2} \end{pmatrix}. \tag{10}$$

The rows of this matrix are mutually orthogonal, so it is used to lower the correlation relationship of the mapped sequences at the input of the FHT. Therefore, the use of this transform reduces the occurrence of the high peaks, compared to the original OFDM frame, adding low computational complexity. This PAPR reduction technique doesn't need side information as, at the receiver side, the transmitted signal is recovered by applying the inverse of the corresponding Hadamard matrix ($\mathbf{H}_N^{-1}$).

3.2. Low complexity PAPR reduction techniques

In <3>, a LC PAPR reduction technique is described for O-OFDM systems based on real valued FFT. Two different symmetries for each transform block are required to implement the scheme. Conversely, here, we use the FHT to implement alternative LC PAPR reduction techniques for O-OFDM without applying any symmetry constraint. The principle of the proposed LC techniques is similar to the standard distortionless PAPR reduction techniques, with the difference that two signal representations of the input signal can be processed in parallel by using a single FHT block, thanks to the properties of this transform <29>. Therefore, the required resources are halved becoming a suitable solution for cost-effective optical implementations. Specifically, in this section we describe the LC-SLM, LC-PTS techniques and LC-SLM with precoding.

3.2.1. Low complexity selective mapping

Low-complexity selective mapping technique, as shown in Fig. 6, consists of creating a complex vector, whose real part carries one signal representation and the imaginary part another representation of the original data. For example, two weighting vectors $\mathbf{P}^{(u)}$, with $u = 1, 2$, are processed by one FHT block combined to be a single input vector $\mathbf{X}^{(1,2)} = [\mathbf{X}\mathbf{P}^{(1)} + j\mathbf{X}\mathbf{P}^{(2)}] = [X_0P_0^{(1)} + jX_0P_0^{(2)}, X_1P_1^{(1)} + jX_1P_1^{(2)}, ..., X_{N-1}P_{N-1}^{(1)} + jX_{N-1}P_{N-1}^{(2)})]$. At the output of the FHT, we obtain a complex vector, $\mathbf{x}^{(1,2)} = FHT\{\mathbf{X}^{(1,2)}\} = FHT\{[\mathbf{X}\mathbf{P}^{(1)} + j\mathbf{X}\mathbf{P}^{(2)}]\} = \mathbf{x}^{(1)} + j\mathbf{x}^{(2)}$. The real part of $\mathbf{x}^{(1,2)}$ is the FHT of

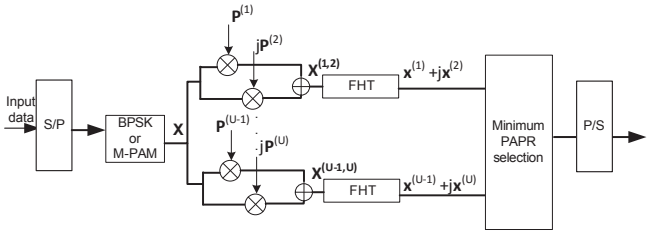

Figure 6: Block diagram of LC-SLM PAPR reduction technique applied to an OFDM transmitter based on the FHT.

the first signal representation and the imaginary part of $\mathbf{x}^{(1,2)}$ is the FHT of the other signal representation. Then the PAPR of both signals is evaluated in order to select the one with minimum peak power. Hence, after the selection process, only a real-valued signal is transmitted. The same scheme is valid for more transform blocks. Adding one FHT results in two new signal representations. Similarly, to SLM, a LC scheme can also be implemented for interleaving technique. Hence, with one FHT block two different signal representations of the transmitted signal can also be processed in parallel. Each signal representation is created with a different interleaver. It will be seen in section 3.3 that both standard techniques have the same performance in terms of PAPR, so we analyze the performance of the LC scheme only for SLM.

3.2.2. Low complexity partial transmit sequences

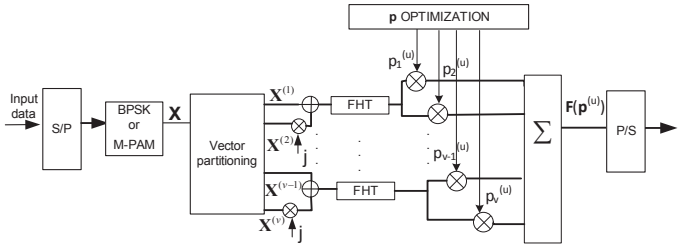

Figure 7: Block diagram of LC-PTS PAPR reduction technique applied to an OFDM transmitter based on the FHT.

In Fig. 7, the block diagram of the proposed technique is depicted. In LC-PTS, as in standard PTS technique, the original data are randomly or adjacently divided into subvectors. Then we construct a complex vector whose real part carries one subvector and the imaginary part carries another.

Both subvectors are parallel processed by one FHT block using half of the resources required by the standard technique. Afterwards the FHT outputs are multiplied by a weighting vector $\mathbf{p}^{(u)}$. Finally, the signal is recombined and the vector $\mathbf{p}^{(u)}$, which has provided the signal with the lowest PAPR is chosen for signal transmission.

3.2.3. Low complexity SLM with precoding

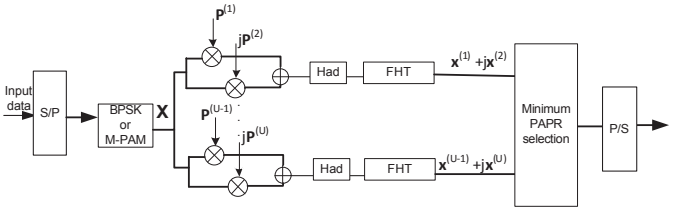

Figure 8: Block diagram of LC-SLM with the Hadamard transform precoding applied to an OFDM transmitter based on the FHT.

The Hadamard transform can be used jointly with other PAPR reduction techniques, such as SLM, to obtain higher reduction of the PAPR. Nevertheless, it must be taken into account for the transponder design that additional transform blocks are used (one at the transmitter for each FHT block and one at the receiver). The signal representations are generated with the LC-SLM scheme and encoded with the Hadamard transform which is performed before implementing the FHT (see Fig. 8). So that, the required Hadamard matrix blocks are halved as well as the FHT blocks.

3.3. Comparison of distortionless PAPR reduction techniques

To evaluate the performance of the proposed PAPR reduction techniques, we analyze the CCDF of the O-OFDM system in Fig.1. The transmitter design is adapted in order to implement the proposed techniques as shown in Figs.4, 5, 6, 7 or 8. Furthermore, for comparison with the FHT-based O-OFDM system, we also analyze the case without applying PAPR reduction techniques when the O-OFDM is based on the FFT. We consider $N = 256$ subcarriers and $L = 4$ oversampling factor. Since real-valued OFDM signals are required, $\mathbf{P}^{(u)}$ and $\mathbf{p}^{(u)}$ vectors have real values in the set $\{\pm 1\}$. Figure 9 shows a number of CCDF curves that are computed for OFDM system implementation cases analyzed in this report. It can be seen that OFDM signals, modulated with either the FFT or the FHT, present the same PAPR

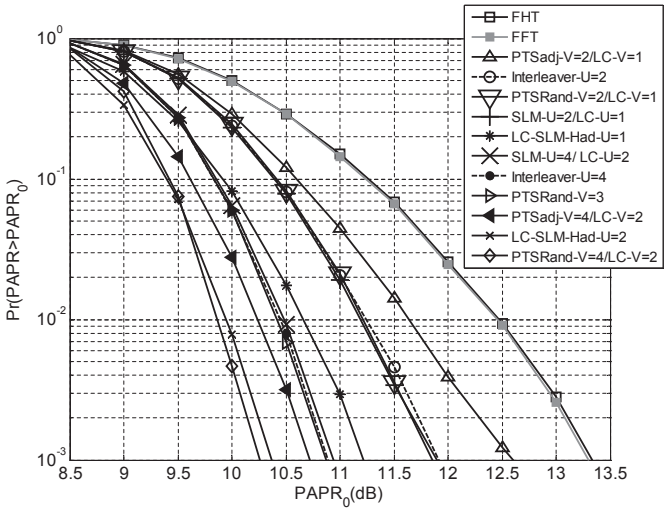

Figure 9: CCDF vs. $PAPR_0$ for OFDM signals (for $N = 256$) with and without standard and LC PAPR reduction techniques.

of 13.3 dB at a CCDF of 0.1%. 2 dB of penalty is obtained, if we compare the achieved result with the PAPR of a complex OFDM signal, according to <30>. LC schemes have the same performance as standard schemes but requires only half transform blocks. In fact, it can be observed that, with $U = 4$ FHT blocks, the standard SLM technique gives a PAPR reduction of 2.4 dB at a probability of 10^{-3}, compared to the unmodified signal PAPR (13.3 dB). The same PAPR reduction is achieved using LC-SLM with $U = 2$ FHT blocks. Using $V = 4$ FHT blocks and applying PTS with adjacent partitions the PAPR reduction is 2.6 dB. PTS with random partitions gives an increased reduction of 3.1 dB. Interleaving technique gives the same performance as SLM using the same number of FHT blocks. The same also occurs in standard OFDM systems based on the FFT, as demonstrated in <11>. It can be also observed that random PTS technique with $V = 3$ blocks gives the same PAPR reduction (2.4 dB) as standard SLM with $U = 4$ transform blocks. Increasing the number of signal representations, better PAPR reduction can be achieved, but it implies using additional transform blocks and this is not suitable for real time applications in optical communications. Hence, we have analyzed the case of using at most 4 FHT blocks corresponding to only 2 FHT for LC schemes. Using SLM, interleaving and PTS random with $U = V = 2$ FHT blocks the probability that the PAPR exceeds 11.8

Table 1: Comparison of PAPR reduction at 10^{-3} CCDF varying the number of FHT blocks at the transmitter for different distortionless techniques

PAPR technique	**1 FHT**	**2 FHT**	**3 FHT**	**4 FHT**
SLM	-	1.5 dB	-	2.4 dB
Interleaver	-	1.5 dB	-	2.4 dB
PTSadj	-	0.7 dB	-	2.6 dB
PTSRand	-	1.5 dB	2.4 dB	3.1 dB
LC-SLM	1.5 dB	2.4 dB	-	-
LC-PTSadj	0.7dB	2.6 dB	-	-
LC-PTSRand	1.5 dB	3.1 dB	-	-

dB is less than 0.1%, resulting in a PAPR reduction of 1.5 dB. The same reduction is obtained with LC-SLM with a single FHT block. Using PTS with adjacent partitions, the reduction is 0.7 dB. Similar difference (in dB) between the PAPR reduction values using PTS and SLM has been obtained in OFDM systems based on the FFT, as demonstrated in <31>. Table 1 summarizes the results that are obtained by applying the proposed PAPR reduction techniques. These results are presented in terms of PAPR reduction that is estimated at CCDF of 0.1%, and at varying number of FHT blocks at the transmitter. We also analyze the LC-SLM technique in combination with the Hadamard transform block for precoding. Firstly, we consider the transmitter design that is shown in Fig. 8 when only one ($U = 1$) FHT block and only one Hadamard transform block is used. In this case the probability that the PAPR is greater than 11.2 dB is less than 0.1%, corresponding to a 2.1 dB reduction compared with the unmodified signal PAPR. When using two FHT blocks ($U = 2$) and two Hadamard transform blocks this reduction is 2.9 dB. It is important to point out that, at the receiver side, only one FHT block is required when applying distortionless PAPR reduction techniques, whereas, with the proposed precoding technique, one additional Hadamard transform block is needed.

4. Performance analysis

In this section, we numerically analyze the performance of the system shown in Fig. 1. We first demonstrate that the same performance is achieved in DMT systems based either on the FFT or FHT. Then, we evaluate the performance of LC-SLM and LC-PTS techniques with random partitions.

In fact, among the techniques described in section 3, LC-SLM and LC-PTS give the highest PAPR reduction when only one or two FHT blocks are used, respectively, without requiring any additional transform block at the receiver. Hence, from now on, as we only evaluate the LC-PTS with random partitions, we will refer to it simply as LC-PTS. When LC-SLM or LC-PTS are implemented, the transmitter shown in Fig. 1 is replaced by the one shown in Fig. 6 with one FHT block or by the transmitter shown in Fig. 7 with two FHT blocks. For the simulation, we consider 6144 OFDM frames with an $N = 256$ FHT points. The clipping and the quantization are modeled according to section 2. The MZM is biased at the quadrature point $V_{bias}/V_{\pi} = -0.5$, where V_{bias} is the bias voltage and V_{π} the switching voltage <24>. As the IM generates an OFDM signal on both sides of the optical carrier frequency, a double-side band (DSB) spectrum is transmitted. Although DD is more robust to dispersion impairments when combined with optical single-side band (SSB) modulation, we use IM with DSB in order to implement a low-cost system, avoiding optical filters or more complex schemes <32>. Furthermore, it has been demonstrated that if IM is performed with an external MZM biased at the quadrature point, the intermodulation products, due to the square law characteristic of the photodetector, are reduced and the guard band can be decreased at the expense of the receiver sensitivity <24; 5>. Here, a guard band equal to the electrical signal bandwidth is considered for correct photodetection. The laser driving the MZM is modeled as a standard continuous wave laser centered at 1550 nm, with output power 1 mW and 10 MHz linewidth, whose phase is modeled as a Wiener process. The optical channel is replaced by a VOA to consider a B2B configuration. The receiver is modeled as an APD with 0.7 A/W responsivity, multiplying factor of 7, overall thermal noise value of 12.87×10^{-12} A/ $\sqrt{Hz}$, and dark current of 1 pA. At the receiver, two noise contributions have been considered: the thermal noise, which is modeled as a Gaussian distribution and the shot noise, which is modeled as a Poisson distribution. The former is due to the photodetector and the electrical amplifier; the latter is due to the photoelectric detection. As the thermal noise dominates over the shot noise, the receiver noise can be assumed to have a Gaussian distribution. Finally, the analog-to-digital conversion is modeled with an electrical digital filter of bandwidth equal to the electrical signal bandwidth <4>. The BER evaluation is performed after the receiver DSP by statistical counting the received bits.

4.1. Sensitivity performance comparison using the FFT and the FHT

The system of Fig. 1 uses the same FHT block in transmission and reception due to the self-inverse property of this transform (as shown in the DSP transmitter and receiver). Whereas, in the case of a standard DMT system, the FFT modulation and demodulation are performed with the inverse fast Fourier transform (IFFT) and the FFT, respectively. The transmitted data are mapped into different constellations depending on the system implementation that we analyze. In order to transmit the same information bit sequence per parallel processing, an M-PAM format (i.e. a real-valued one-dimensional constellation) must be used with the FHT while a two dimensional M^2 quadrature-amplitude modulation (M^2-QAM) format is required with the FFT, due to the HS constraint. When the FFT is used, only half of the total electrical signal bandwidth is filled with data, as the other half is used to transmit the symmetric redundant symbols. In the case of FHT processing, the entire bandwidth is used to transmit useful information. Therefore, the same spectral efficiency and bit optical power are obtained using the FHT with BPSK, 4-PAM and 8-PAM formats and using the FFT with 4-QAM, 16-QAM and 64-QAM formats, respectively, as demonstrated in <9>. Figure 10 shows the B2B sensitivity performance of FHT- and FFT-based systems for different constellation sizes. In the simulations, a

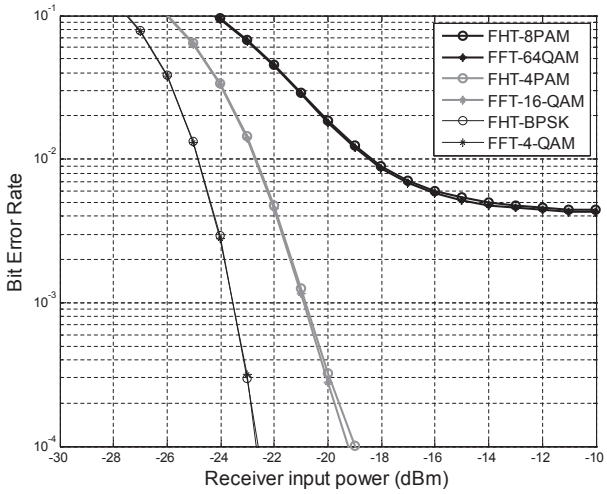

Figure 10: Sensitivity performance comparison of DD O-OFDM system based on FFT and FHT.

randomly generated stream of bits transmitted at 10 Gb/s is considered. A

finite DAC resolution of 8 bits and a clipping level of 7 dB are considered in order to take into account the quantization and clipping noise. In Fig. 10, it can be seen that both the transforms have the same sensitivity performance. Using the FHT with BPSK format, a receiver input power of -23.55 dBm is needed to ensure a BER of 10^{-3}. The same receiver input power is required to achieve the same target BER with the FFT and 4-QAM format. Using 4-PAM format and the FHT or 16-QAM with the FFT, the required receiver power is 2.65 dB higher to guarantee 10^{-3} BER. Using either the FHT with 8-PAM format or the FFT with 64-QAM format, a 7 dB clipping level is not enough to ensure a target BER of 10^{-3}, and both the BER curves present a floor above this value.

4.2. PAPR reduction impact on the system performance

According to <33> and the results shown in Fig. 10, quantization and clipping noise severely degrade the OFDM signal when high modulation formats, such as 8-PAM, are used. Therefore, we analyze the case of O-OFDM system using this modulation format, for a bit rate of 15 Gb/s. We evaluate the BER performance of the system with and without the proposed LC PAPR reduction techniques, which halve the required number of FHT blocks at the transmitter.

4.2.1. Clipping noise analysis

Figure 11 shows the BER performance of the B2B O-OFDM system of Fig. 1 for different clipping levels. We have analyzed the B2B configuration for a fixed receiver input power of -17 dBm and considering an ideal DAC. Using LC-PTS with 2 FHT blocks at constant receiver power (-17 dBm) and with a clipping level of 7.4 dB, a target BER of 10^{-3} is achieved. Additionally, using a single FHT block with LC-SLM, a target BER of 10^{-3} can be obtained with a clipping level of 8.2 dB. When LC PAPR reduction techniques are not applied, this target BER cannot be achieved with this receiver input power.

4.2.2. Quantization noise analysis

The clipping level is fixed to 9 dB in order to evaluate the influence of the quantization noise. In fact, in <3>, it is demonstrated that 9 dB is the optimum clipping level when using the FFT with 64-QAM, which corresponds to 8-PAM format when the FHT is used <9>. Figure 12 shows the BER performance for a fixed receiver input power of -17 dBm varying when the DAC bit resolution is varying in the range from 4 bits to 8 bits. Applying

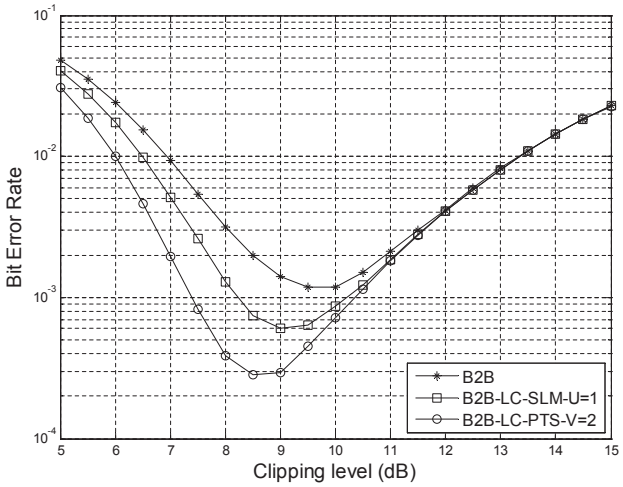

Figure 11: BER performance in B2B configuration at a constant receiver input power of -17 dBm versus clipping level for 8-PAM O-OFDM ($N = 256$) with and without LC PAPR reduction techniques.

LC-PTS with 2 FHT blocks a target BER of 10^{-3} can be ensured using a DAC of 6 bit resolution. With LC-SLM, using a single FHT block, the same BER is guaranteed for a DAC of 7 bits. When no PAPR techniques are applied, a BER of 10^{-3} cannot be obtained for this receiver input power.

4.2.3. Sensitivity performance

Figure 13 shows the B2B sensitivity performance of the system of Fig. 1 with and without the proposed LC-SLM and LC-PTS schemes. The receiver input power is measured for a fixed BER of 10^{-3}, varying both the clipping level and the number of bits resolution of the DAC. Applying the proposed techniques, thanks to the mitigation of both the PAPR and clipping noise, the clipping level required to ensure a target BER of 10^{-3} is reduced and the receiver sensitivity is enhanced. Using LC-PTS with 2 FHT blocks and for DAC resolutions of 6 and 8 bits, a clipping level of 7 dB is enough to guarantee 10^{-3} BER. Applying LC-SLM with a single FHT block and for 8 bit DAC resolution, a minimum clipping level of 7.3 dB is needed to ensure the same target BER. Using a DAC of 6 bit resolution the minimum clipping level is increased by 0.1 dB. Whereas, in the case of not applying techniques, the required clipping level must be at least 7.9 dB when a DAC of 8 bits is used or 8 dB for a 6 bit DAC resolution. The receiver input power corresponding

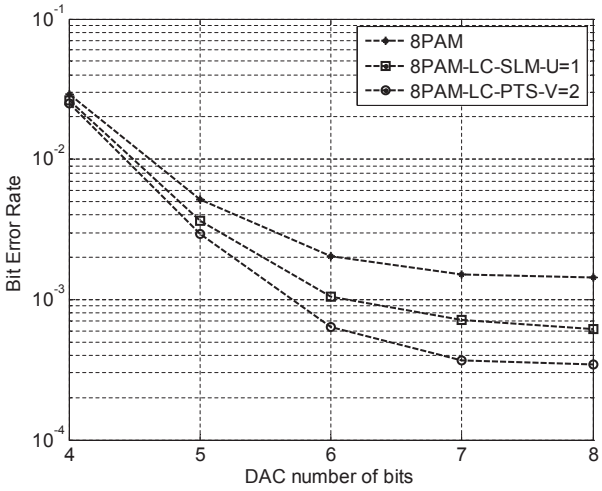

Figure 12: BER performance at a constant receiver input power of -17 dBm versus the number of bits of the DAC for 8-PAM O-OFDM based on the FHT ($N = 256$) with and without LC PAPR reduction techniques. (Dashed lines are drawn for a better visualization of the figure.)

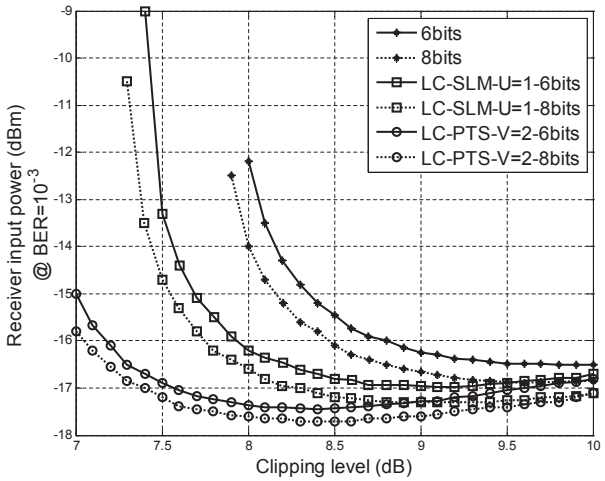

Figure 13: Sensitivity performance at a target BER of 10^{-3} for 8-PAM O-OFDM system based on the FHT affected by clipping and quantization noise varying the clipping level and using 6 and 8 bit DAC resolutions.

to 9 dB clipping level and 8 bit DAC, without PAPR reduction, is -17.7 dBm. By applying the proposed techniques, the clipping level required to

obtain the same receiver input power is reduced. Specifically, 1 dB and 1.8 dB reduction are obtained, when LC-SLM with a single FHT and LC-PTS with 2 FHT are respectively applied. The clipping noise impact is higher for low values of clipping level. With 8 dB clipping level and compared to the case of not using techniques, for 8 bit DAC resolution, it is demonstrated that applying LC-SLM, the required receiver power for 10^{-3} BER is 2.6 dB lower than the case of not using techniques. Applying LC-PTS with 2 FHT blocks, the reduction is 3.6 dB. Using a 6 bit DAC, the required receiver power decreases 4 dB when LC-SLM is applied and of 5.1 dB when LC-PTS is implemented.

5. Conclusion

In this paper, we have analyzed standard distortionless PAPR reduction techniques based on the FHT and proposed low complexity schemes. Thanks to the FHT properties, a simplified DSP can be used and LC techniques can be easily applied without any symmetry constraint. Applying LC-SLM without any additional transform block at the transmitter, a PAPR reduction of 1.5 dB is obtained. The proposed LC-PTS with random partitions allows achieving the highest PAPR reduction of 3.1 dB using only one additional transform block. We have demonstrated that applying LC PAPR reduction techniques in DD O-OFDM systems based on the FHT, the quantization and the clipping noise are mitigated and the required number of resources is halved. The performance of the system is improved in terms of receiver sensitivity and power efficiency. At the same time, the constraints on the linear dynamic range of DAC/ADC, drivers and modulators are relaxed thanks to both the symmetrically clipping and PAPR reduction. Furthermore, applying LC PAPR reduction techniques, the required clipping level to guarantee a target BER of 10^{-3} for fixed receiver input power is reduced. Finally, we have shown that, for a B2B configuration and using a 6 bit DAC, the required receiver power is 4 dB and 5.1 dB lower, when LC-SLM with a single FHT block and LC-PTS with one additional block are respectively applied.

Acknowledgment

This work was founded by the MINECO (Economy and competitiveness Ministry of Spain) through the project FARO (TEC2012-38119), by the EU-FP7 integrated project IDEALIST (GA no. 317999), the FPI research scholarship grant BES-2010-031072 and the grant PTQ-11-04805.

[1] W. Shieh, I. Djordjevic, OFDM for Optical Communications, Elsevier,USA, 2010.

[2] J. Armstrong, OFDM for optical communications, Journal of Lightw. Technol. volume 27 (2009) pp. 189–204.

[3] S. C. J. Lee, F. Breyer, S. Randel, H. P. A. van den Boom, A. M. J. Koonen, High-speed transmission over multimode fiber using discrete multitone modulation, J. Opt. Netw. volume 7 (2008) pp.183–196.

[4] M. Svaluto Moreolo, R. Munoz, G. Junyent, Novel power efficient optical OFDM based on hartley transform for intensity-modulated direct-detection systems, J. Lightw.Technol. volume 28 (2010) pp.798 –805.

[5] M. Svaluto Moreolo, J. M. Fabrega, F. J. Vilchez, L. Nadal, G. Junyent, Experimental demonstration of a cost-effective bit rate variable intensity modulation and direct detection optical OFDM with reduced guard band, in: ECOC, P3.17, 2012.

[6] C. Wang, C. Chang, J. Fan, J. Cioffi, Discrete Hartley transform based multicarrier modulation, in: ICASSP, volume 5, 2000, pp. 2513 – 2516.

[7] C.-L. Wang, C.-H. Chang, A DHT-based FFT/IFFT processor for VDSL transceivers, in: ICASSP, volume 2, 2001, pp. 1213 –1216.

[8] D. Wang, D. Liu, F. Liu, G. Yue, A novel DHT-based ultra-wideband system, in: ISCIT, volume 50, 2005, pp. 172–184.

[9] M. Svaluto Moreolo, Performance analysis of DHT-based optical OFDM using large-size constellations in AWGN, IEEE Comm.Lett. volume 15 (2011) pp.572 –574.

[10] E. Vanin, Performance evaluation of intensity modulated optical OFDM system with digital baseband distortion, Opt. Exp. volume 19 (2011) pp.4280–4293.

[11] S. H. Han, J. H. Lee, An overview of peak-to-average power ratio reduction techniques for multicarrier transmission, IEEE Wireless Comm. volume 12 (2005) pp.56 – 65.

[12] B. Goebel, S. Hellerbrand, N. Haufe, N. Hanik, PAPR reduction techniques for coherent optical OFDM transmission, in: ICTON, 2009, pp. 1 –4.

[13] M. El Tabach, P. Tortelier, R. Pyndiah, O. Bouchet, On free-space optic communication with alamouti-type coding and direct detection, in: Int. Symp. on Wireless Perv. Comp., 2008, pp. 740 –743.

[14] J.-K. Sang-Woo, Heung-Gyoon, PAPR reduction of the OFDM signal by the SLM-based WHT and DSI method, in: IEEE TENCON, 2006, pp. 1 –4.

[15] I. Baig, V. Jeoti, DCT precoded SLM technique for PAPR reduction in OFDM systems, in: ICIAS, 2010, pp. 1 –6.

[16] B. Krongold, Y. Tang, W. Shieh, Fiber nonlinearity mitigation by PAPR reduction in coherent optical OFDM systems via active constellation extension, in: ECOC, 2008, pp. 1 –2.

[17] L. Nadal, M. Svaluto Moreolo, J. M. Fabrega, G. Junyent, Comparison of peak power reduction techniques in optical OFDM systems based on FFT and FHT, in: ICTON, We.A1.5, 2011.

[18] L. Chen, B. Krongold, J. Evans, A tone reservation-based optical OFDM system for short-range IM/DD transmission, J. of Lightw. Technol. volume 29 (2011) pp.3824 –3833.

[19] E. Vanin, Signal restoration in intensity-modulated optical ofdm access systems, Opt. Lett. volume 36 (2011) pp.4338–4340.

[20] B. Ranjha, M. Kavehrad, Precoding techniques for PAPR reduction in asymmetrically clipped OFDM based optical wireless system, in: SPIE, volume 8645, 2013, pp. 86450R–86450R–9.

[21] M. S. Moreolo, J. M. Fàbrega, F. J. Vílchez, L. Nadal, G. Junyent, Experimental demonstration of a cost-effective bit rate variable IM/DD optical OFDM with reduced guard band, Opt. Express 20 (2012) B159–B164.

[22] H. Taga, A theoretical study of OFDM system performance with respect to subcarrier numbers, Opt. Exp. vol.17 (2009) pp.18638–18642.

[23] C. Tellambura, Computation of the continuous-time PAR of an OFDM signal with BPSK subcarriers, IEEE Comm. Lett. volume 5 (2001) pp.185 –187.

[24] J. Leibrich, A. Ali, H. Paul, W. Rosenkranz, K.-D. Kammeyer, Impact of modulator bias on the OSNR requirement of direct-detection optical OFDM, IEEE Photon. Technol. Lett. volume 21 (2009) pp.1033 –1035.

[25] R. Buml, R. F. H. Fischer, J. B. Huber, Reducing the peak-to-average power ratio of multicarrier modulation by selected mapping, Electron. Lett. volume 32 (1996) pp.2056–2057.

[26] A. Jayalath, C. Tellambura, Reducing the peak-to-average power ratio of orthogonal frequency division multiplexing signal through bit or symbol interleaving, Electron. Lett. volume 36 (2000) pp.1161 –1163.

[27] S. Muller, J. Huber, OFDM with reduced peak-to-average power ratio by optimum combination of partial transmit sequences, Electron. Lett. volume 33 (1997) pp.368 –369.

[28] S. Muller, J. Huber, A novel peak power reduction scheme for OFDM, in: IEEE Int. Symp. on Pers., Indoor and Mobile Radio Comm.,PIMRC,, volume 3, 1997, pp. 1090 –1094.

[29] M. Svaluto Moreolo, L. Nadal, J. M. Fabrega, G. Junyent, FHT-based architectures for multicarrier modulation in direct detection and coherent optical systems, in: ICTON, We.A1.1, 2011.

[30] S. A. Aburakhia, E. F. Bradan, D. A. Mohamed, Distribution of the PAPR for real-valued OFDM signals, in: International Conference on Information Technology (ICIT), 2009.

[31] S. H. Muller, J. B. Huber, A comparison of peak power reduction schemes for OFDM, IEEE Global Telecommunications Conference (GLOBECOM) (1997) pp. 1–5.

[32] B. Schmidt, A. Lowery, J. Armstrong, Experimental demonstrations of electronic dispersion compensation for long-haul transmission using direct-detection optical OFDM, J. Lightw. Technol. volume 26 (2008) pp.196 –203.

[33] L. Nadal, M. Svaluto Moreolo, J. M. Fabrega, G. Junyent, Clipping and quantization noise mitigation in intensity-modulated direct detection O-OFDM systems based on the FHT, in: ICTON, We.B1.5, 2012.